

Chapter 6

Behavior and Electrocatalytic Degradation of Textile Azo Dye Under Acidic Conditions



Sanaa El Aggadi , Amale Boutakiout, Mariem Ennouhi, Aicha Chadil, and Abderrahim El Hourch

Abstract The decomposition of textile azo dye Violet 5R in H₂SO₄ (1 M) solution was investigated by electrochemical method. Electrochemical behavior of dye was realized with cyclic voltammetry (CV). A conventional three-electrode cell was employed to study a dye concentration and potential scan rate effect, with the platinum (Pt) electrode employed as the working electrode. The potential chosen for the azo dye was between -0.24 V/SCE to 1.5 V/SCE. A linear relationship was found between the square root of the potential scan rate ($v^{1/2}$) and the current density. Such behavior appears characteristic of a diffusion-controlled process. Charge transfer coefficient (α) and the diffusion coefficient (D) were calculated and were found to be 0.49 and 1.84×10^{-5} cm².s⁻¹, respectively. The electrochemical treatment of the Violet 5R dye in H₂SO₄ solution was performed using the chronoamperometry method by imposing a potential of 1.5 V/SCE for 2 h. The voltammograms before and after electrolysis show a decrease of the current density of anodic peaks after electrolysis. The efficiency of dye removal in the acidic electrolyte achieved 65% after 2 h of electrolysis using the chronoamperometric technique.

Keywords Violet 5R · Cyclic voltammetry · Electrooxidation · Diffusion coefficient · Chronoamperometry · Azo dyes

6.1 Introduction

Large quantities of wastewater with various types of reactive dyes are released from the textile industry. Such substances cause not only wastewater pollution, but also lead to an increase in the concentration of chemical oxygen demand (COD) over the limits allowed by the current regulations (Khellouf et al. 2020; Swati and Faruqui 2018). Azo dyes are the most commonly used dyes in the textile industry, they represent between 60 and 70% of all kinds of used dyes (Carliell et al. 1998). Azo dyes in

S. El Aggadi (✉) · A. Boutakiout · M. Ennouhi · A. Chadil · A. El Hourch
Department of Chemistry, Faculty of Sciences, Mohammed V University in Rabat, 4 Avenue Ibn Battouta, BP:1014, Rabat, Morocco
e-mail: sanaa_elaggadi@um5.ac.ma

6.2 Experimental

Displayed equations are centered and set on a separate line. A three-electrode cell with a Pt electrode (0.2 cm^2) serving as the working electrode (WE), glassy carbon acting as the counter electrode (CE), and a saturated calomel electrode (SCE) as the reference electrode (RE) were used for electrochemical oxidation. Measurements of cyclic voltammetry and chronoamperometry were conducted by means of a PGZ 301 potentiostat/galvanostat that is controlled by the VoltMaster 4 software. Violet 5R was obtained from OH YOUNG INDUSTRIAL CO. LTD. Sulfuric acid (96%, Sigma-Aldrich) was employed for electrolyte ($1 \text{ M H}_2\text{SO}_4$) preparation. All solutions are made using ultrapure water. Prior to all scans, and to provide a reproducible surface, the electrode was prepared by polishing, the electrode was prepared to provide a reproducible surface by polishing, rinsing with distilled water, and then cleaned electrochemically by CV in a $1 \text{ M H}_2\text{SO}_4$ solution until obtaining a reproducible voltammogram. All electrochemical investigations were carried out at room temperature ($25 \text{ }^\circ\text{C}$).

6.3 Results and Discussion

6.3.1 Influence of Violet 5R Dye Concentration

The cyclic voltammograms recorded for various concentrations between 0.5 and 10 mM of Violet 5R dye during cycling in the potential area from -0.24 to 1.5 V/SCE in H_2SO_4 (1 M) solution at a scan rate of 50 mV/s are shown in Fig. 6.1. The voltammetric curve of the dye shows, for all concentrations, the presence of anodic peaks at 0.42 V/SCE , 0.75 V/SCE and 1.33 V/SCE in forward sweep and cathodic peaks at 1.14 V/SCE , 0.46 V/SCE and -0.08 V/SCE in reverse scan. An oxidation and reduction peak were observed just for the 5 mM and 10 mM concentrations. According to this figure, it can be easily observed that when the concentration of Violet 5R dye increases, the current density of the anodic peaks increases and their position moves to the highest potential levels.

The obtained voltammograms demonstrate that it is possible to detect even millimolar concentrations of dye. Figure 6.2a displays the oxidation peaks current density plotted against Violet 5R concentration. The peak current density increases when the concentration of Violet 5R increases, with a linear variation ($R^2 = 0.98$). Figure 6.2b shows the evolution of the peak potential versus the logarithm of Violet 5R concentration. The anodic peak potential is linearly varied with respect to the logarithm of Violet 5R concentration ($R^2 = 0.98$).

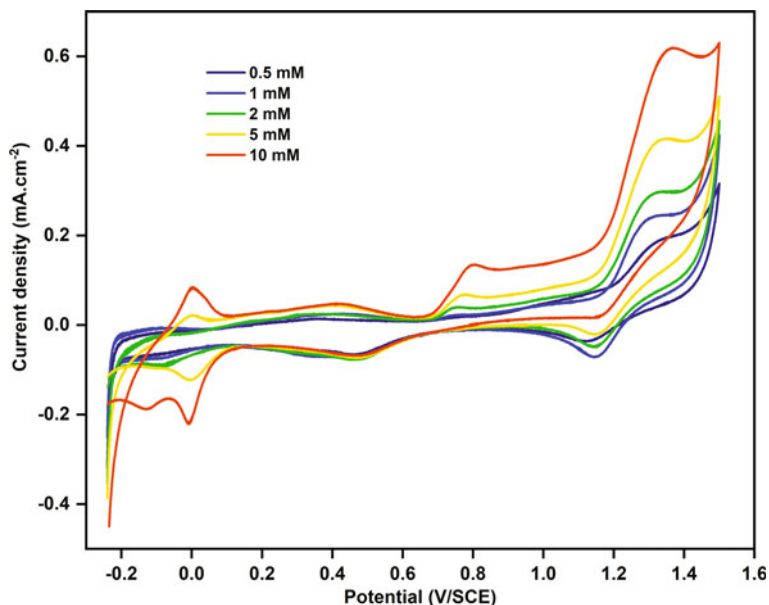


Fig. 6.1 Cyclic voltammograms plotted with the Pt electrode at a potential scan rate of 50 mV/s for various concentrations of Violet 5R dye in 1 M H₂SO₄

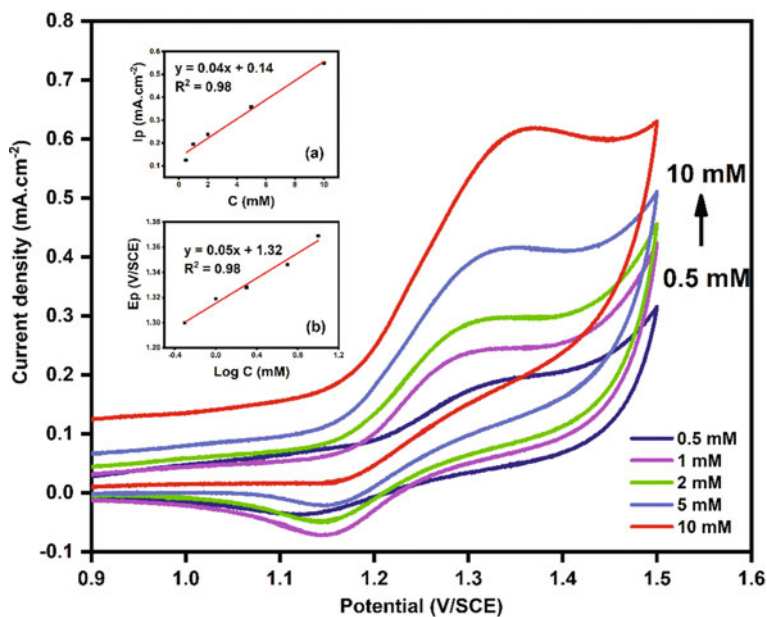


Fig. 6.2 Cyclic voltammograms for the oxidation of Violet 5R at various concentrations, **a** Dependence of the oxidation peak current density versus concentration, **b** Evolution of the oxidation peak potential as function of log (C)

6.3.2 Influence of Potential Scan Rate

From the relation between scan rate (v) and peak current, constructive information is obtained about the electro-chemical process. The electrochemical behavior of Violet 5R at various scan rates was explored through the use of cyclic voltammetry method from 20 to 500 mV/s recorded at Pt working electrode for 1 M H_2SO_4 and 10 mM of Violet 5R (See Fig. 6.3). An increase in the scan rates led to an increase in the anodic peak currents (I_{pa}) and the peak potential (E_p) moves to the highest potential levels. A possible explanation for this behavior is that species are depleted near the Platinum surface when sufficient potential is imposed on the Pt- surface leading to species oxidation in the solution (Sayyah et al. 2014).

The peak currents for the anodic oxidation of Violet 5R dye were proportional to the square root of the scan rate ($v^{1/2}$) over the range 20–500 mV/s as shown in Fig. 6.3a (inset). This result demonstrates that up to the scan rate = 500 mV/s, the reaction is controlled by the diffusion of Violet 5R (Gowda and Nandibewoor 2014), and the formula can be written as follows:

$$I_p \text{ (mA)} = 1.80v^{1/2} \text{ (V/s)}^{1/2} + 0.16, \quad (R^2 = 0.99) \quad (6.1)$$

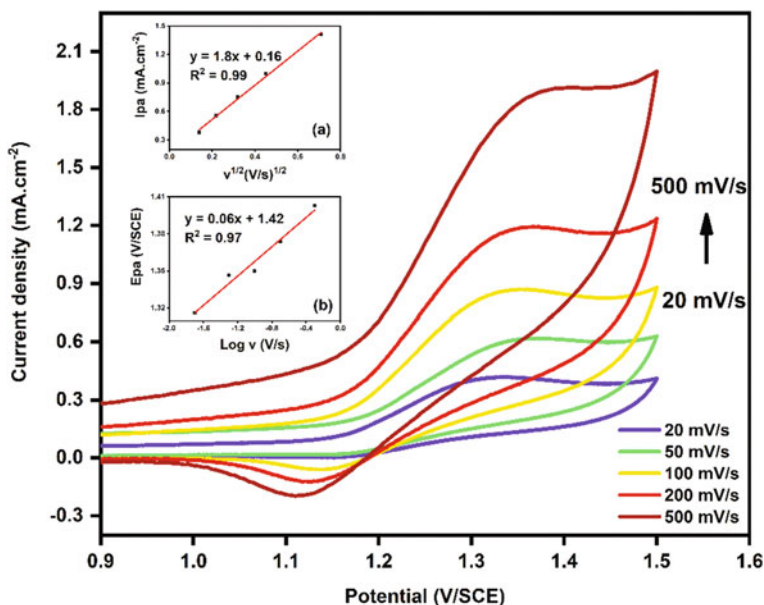


Fig. 6.3 Cyclic voltammograms recorded at different potential scan rate (v) (20–500 mV/s) of violet 5R dye (10 mM) in 1 M H_2SO_4 , **a** Evolution of the oxidation peak current density as function of $v^{1/2}$, **b** Evolution of the oxidation peak potential as function of $\log v$

The E_p of the oxidation peak was also a function of the scan rate. By increasing the scan rate, the peak potential moved to more positive values, indicating the irreversibility of the oxidation mechanism, and the following equation can be used to express a linear relationship between the peak potential and the logarithm of the scan rate (See Fig. 6.3b):

$$E_p (V) = 0.06 \log v (V/s) + 1.42, (R^2 = 0.97) \quad (6.2)$$

Furthermore, a straight line of the Tafel plot between the E_p and the logarithm of the scan rates is shown in the lower inset of Fig. 6.3. The linear formula is given as follows: $E_p = 0.06 \log v + 1.42, R^2 = 0.97$.

In order to determine the diffusion coefficient, we use the peak current density I_p of cyclic voltammetry curve for an irreversible process, expressed as (Wei et al. 2022):

$$I_p = 0.4958 \times nF(\alpha nF/RT)^{1/2} \times A \times C \times D^{1/2} \times v^{1/2} \quad (6.3)$$

where:

- D: Diffusion coefficient;
- n: Number of electrons transferred;
- T: Temperature;
- C: Initial concentration of Violet 5R;
- α : Charge transfer coefficient;
- A: Active surface area of the WE;
- R: Ideal gas constant;
- F: Faraday's constant;
- V: Potential scan rate.

α can be found from the following equation:

$$E_p = 0.5b \log v + K \quad (6.4)$$

With:

- B: Tafel slope;
- K: Potential intercept.

Based on Eq. (6.3), the slope of $E_p = f(\text{Log } v)$ is:

$$dE_p/d\log v = b/2 \quad (6.5)$$

With:

$$b = 2.3RT/\alpha nF \quad (6.6)$$

Form the slope of the linear evolution of E_p with $\text{Log } v$ from data exhibited in Fig. 6.3b, the α value can be found utilizing Eq. (6.6). With the α values, the diffusion coefficient D of Violet 5R is determined by the slope of the right lines depicted in

Fig. 6.3a through the use of Eq. (6.3). The deduced values of α and D of Violet 5R are 0.49 and $1.84 \times 10^{-5} \text{ cm}^2 \cdot \text{s}^{-1}$.

6.3.3 Electrolysis of Violet 5R Dye by Chronoamperometry

Chronoamperometry experiment was carried out at a constant potential of 1.5 V/SCE during 2 h of electrolysis in a solution containing 10 mM of Violet 5R in 1 M H_2SO_4 (See Fig. 6.4). The plots depict a typical current drop within the first seconds related to the oxidation of Violet 5R on the Pt electrode by applying 1.5 V/SCE, succeeded by a smaller change with respect to time, attributed to the oxidation of Violet 5R at equilibrium conditions. In Fig. 6.4 (Insert), we found a linear dependence between $t^{-1/2}$ and I the current density. This means that the transient current must be controlled by a diffusion process (Li et al. 2020). According to the graph, the current stabilizes after a nucleation phase. The curve therefore reflects the degradation of Violet 5R dye in H_2SO_4 . Indeed, the color of the solution is becoming more and more pastel.

We plotted voltammograms of Violet 5R in H_2SO_4 before and after electrolysis. We can observe that the cyclic voltammogram taken after 2 h of electrolysis showed a pronounced diminution of the oxidation peak of Violet 5R dye as well as the color

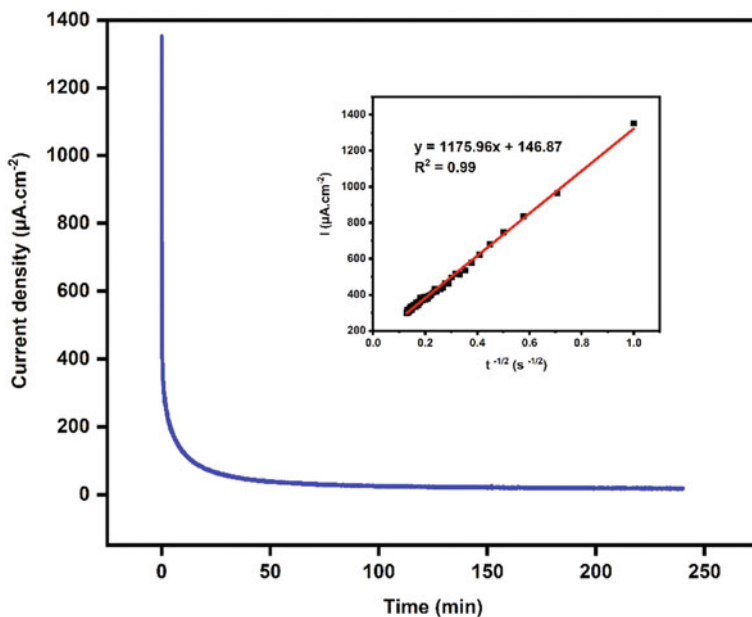


Fig. 6.4 Chronoamperometry plot of Violet 5R dye (10 mM) dissolved in H_2SO_4 (1 M) solution for 2 h at 1.5 V/SCE. *Insert:* I versus $t^{-1/2}$

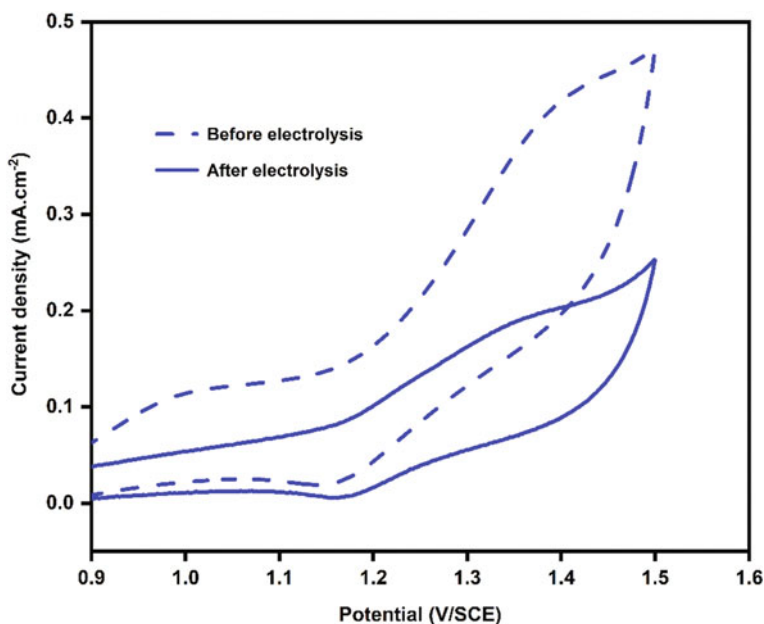


Fig. 6.5 Cyclic voltammograms registered prior and after the electrolysis process of Violet 5R dye (10 mM) using 50 mV/s

of the solution becomes paler (See Fig. 6.5). It can be said that the concentration of Violet 5R dye in H₂SO₄ has decreased, which shows that there is a degradation of the dye after electrolysis.

The % of dye elimination was calculated using the formula (Anantha et al. 2020):

$$R(\%) = \frac{C_0 - C}{C_0} * 100\% \quad (6.7)$$

where:

C₀: Concentrations of the dye before electrolysis (mol.L⁻¹);

C: Concentrations of the dye after electrolysis (mol.L⁻¹).

The dye removal efficiency is 65% after 2 h of electrolysis in H₂SO₄ medium at room temperature.

6.4 Conclusion

At room temperature, the decolorization of textile azo dye Violet 5R in H₂SO₄ was realized by the electro-chemical degradation, the process was performed in a three-electrode cell at constant potential with a Pt wire used as WE. A strong relationship

between the peak current density (I) and Violet 5R dye concentration, as the dye concentration increases with a linear variation ($R^2 = 0.98$), the peak current density increases, it means that Violet 5R easily oxidizes on the Pt electrode surface. The electrocatalytic oxidation of dye is affected significantly by faster potential scan rates. The charge transfer coefficient (α) and the diffusion coefficient (D) were calculated and found to be 0.49 and $1.84 \times 10^{-5} \text{ cm}^2 \cdot \text{s}^{-1}$ respectively. The percent of color removal in acid environment is 65% after 2 h of electrolysis. The global experimental results show that the electrochemical process is able to be employed as a pretreatment step before conventional treatment.

References

- Anantha MS, Olivera S, Hu C, Jayanna BK, Reddy N, Venkatesh K, Muralidhara HB, Naidu R (2020) Comparison of the photocatalytic, adsorption and electrochemical methods for the removal of cationic dyes from aqueous solutions. *Environ Technol Innov* 17:100612
- Aminuzzaman M, Chong CY, Goh WS, Phang YK, Lai-Hock T, Chee SY, Akhtaruzzaman M, Ogawa S, Watanabe A (2020) Biosynthesis of NiO nanoparticles using soursop (*Annona muricata* L.) fruit peel green waste and their photocatalytic performance on crystal violet dye. *J Clust Sci* 1–10
- Albahnasawi A, Yüksel E, Gürbulak E, Duyum F (2020) Fate of aromatic amines through decolorization of real textile wastewater under anoxic-aerobic membrane bioreactor. *J Environ Chem Eng* 8:104226
- Ayed L, Bekir K, Achour S, Cheref A, Bakhrouf A (2017) Exploring bioaugmentation strategies for azo dye CI Reactive Violet 5 decolorization using bacterial mixture: dye response surface methodology. *Water Environ J* 31:80–89
- Carliell CM, Barclay SJ, Shaw C, Wheatley AD, Buckley CA (1998) The effect of salts used in textile dyeing on microbial decolourisation of a reactive azo dye. *Environ Technol (United Kingdom)* 19:1133–1137
- Clematis D, Panizza M (2021) Application of boron-doped diamond electrodes for electrochemical oxidation of real wastewaters. *Curr Opin Electrochem* 30:100844
- El Aggadi S, El Abbassi Z, El Hourch A (2021a) Color removal from dye-containing aqueous solutions by electrooxidation. *Desalin Water Treat* 215:232–236
- El Aggadi S, Kaichouh G, El Abbassi Z, Fekhaoui M, El Hourch A (2021b) Electrode material in electrochemical decolorization of dyestuffs wastewater: a review. In: *E3S web of conferences*
- El Aggadi S, El Hourch A (2021) Removal of reactive blue 21 (RB21) phthalocyanine dye from aqueous solution by adsorption process: a review. *Polish J Environ Stud* 30:3425–3432
- Escalona-Durán F, Villegas-Guzman P, dos Santos EV, da Silva DR, Martínez-Huitile CA (2019) Intensification of petroleum elimination in the presence of a surfactant using anodic electrochemical treatment with BDD anode. *J Electroanal Chem* 832:453–458
- El-Defrawy MM, Kenawy IMM, ZAKI E, El-tabey RM (2019) Adsorption of the anionic dye (Diamond Fast Brown KE) from textile wastewater onto chitosan/montmorillonite nanocomposites. *Egypt J Chem* 62:13–14
- El Fawal G, Ibrahim A, Akl M (2019) Methylene blue and crystal violet dyes removal (as a binary system) from aqueous solution using local soil clay: kinetics study and equilibrium isotherms. *Egypt J Chem* 62:541–554
- El-Khawaga AM, Farrag AA, Elsayed MA, El-Sayyad GS, El-Batal AI (2021) Promising antimicrobial and azo dye removal activities of citric acid-functionalized magnesium ferrite nanoparticles. *J Clust Sci* 1–17
- Gowda JI, Nandibewoor ST (2014) Electrochemical behavior of paclitaxel and its determination at glassy carbon electrode. *Asian J Pharm Sci* 9:42–49

- Jing X, Yuan J, Cai D, Li B, Hu D, Li J (2021) Concentrating and recycling of high-concentration printing and dyeing wastewater by a disc tube reverse osmosis-Fenton oxidation/low temperature crystallization process. *Sep Purif Technol* 266:118583
- Kaur H, Kaur S, Kumar S, Singh J, Rawat M (2020) Eco-friendly approach: synthesis of novel green TiO₂ nanoparticles for degradation of reactive green 19 dye and replacement of chemical synthesized TiO₂. *J Clust Sci* 1–14
- Khellouf M, Chemini R, Salem Z, Khodja M, Zeriri D, Jada A (2020) A new activated carbon prepared from cypress cones and its application in the COD reduction and colour removal from industrial textile effluent. *Environ Dev Sustain* 1–16
- Liu Y, Huang L, Mahmud S, Liu H (2020) Gold nanoparticles biosynthesized using ginkgo biloba leaf aqueous extract for the decolorization of azo-dyes and fluorescent detection of Cr(VI). *J Clust Sci* 31:549–560
- Li C, Li S, Che Y, Li J, Shu Y, He J, Song J (2020) Electrochemical behavior of niobium ions in molten KCl-NaCl. *J Mater Res Technol* 9:9341–9347
- Luo X, Liang C, Hu Y (2019) Comparison of different enhanced coagulation methods for azo dye removal from wastewater. *Sustainability* 11:4760
- Mishra S, Nayak JK, Maiti A (2020) Bacteria-mediated bio-degradation of reactive azo dyes coupled with bio-energy generation from model wastewater. *Clean Technol Environ Policy* 22(22):651–667
- Nabizadeh Chianeh F, Avestan MS (2020) Application of central composite design for electrochemical oxidation of reactive dye on Ti/MWCNT electrode. *J Iran Chem Soc* 17:1073–1085
- Pirkarami A, Fereidooni L (2019) Titanium electrode modified by nano-PMDAH as a highly efficient polymer for removal of reactive red 13 using solar cells for energy-harvesting applications. *J Iran Chem Soc* 16:851–864
- Rafaqat S, Ali N, Torres C, Rittmann B (2022) Recent progress in treatment of dyes wastewater using microbial-electro-Fenton technology. *RSC Adv* 12:17104–17137
- Sayyah SM, Abd-Elrehim SS, Azooz RE, Mohamed F (2014) Electrochemical study of the copolymer formation between o-chlorophenol and o-hydroxyphenol. *J Korean Chem Soc* 58:289–296
- Sonal S, Mishra BK (2021) Role of coagulation/flocculation technology for the treatment of dye wastewater: trend and future aspects. *Water Pollut Manag Pract* 303–331
- Swati SS, Faruqui AN (2018) Investigation on ecological parameters and COD minimization of textile effluent generated after dyeing with mono and bi-functional reactive dyes. *Environ Technol Innov* 11:165–173
- Thangaraj S, Bankole PO, Sadasivam SK (2021) Microbial degradation of azo dyes by textile effluent adapted, enterobacter hormaechei under microaerophilic condition. *Microbiol Res* 250:126805
- Titus D, Samuel EJJ (2019) Photocatalytic degradation of azo dye using biogenic SnO₂ nanoparticles with antifungal property: RSM optimization and kinetic study. *J Clust Sci* 30:1335–1345
- Unnisa A, Abouzied AS, Baratam A, Lakshmi KNVC, Hussain T, Kunduru RD, Banu H, Fatima SB, Hussian A, Selvarajan KK (2020) Design, synthesis, characterization, computational study and in-vitro antioxidant and anti-inflammatory activities of few novel 6-aryl substituted pyrimidine azo dyes. *Arab J Chem* 13:8638–8649
- Wang AJ, Wang HC, Cheng HY, Liang B, Liu WZ, Han JL, Zhang B, Wang S (2020) Sen: Electrochemistry-stimulated environmental bioremediation: development of applicable modular electrode and system scale-up. *Environ Sci Ecotechnology* 3:100050
- Wei X, Wang G, Li F, Zhang J, Chen J, Wang R (2022) High performance positive electrolyte with potassium diformate (KDF) additive for vanadium redox flow batteries. *Int J Electrochem Sci* 17:2
- Yu X, Liu H, Diao J, Sun Y, Wang Y (2018) Magnetic molecularly imprinted polymer nanoparticles for separating aromatic amines from azo dyes—synthesis, characterization and application. *Sep Purif Technol* 204:213–219
- Zhang C, Chen H, Xue G, Liu Y, Chen S, Jia C (2021) A critical review of the aniline transformation fate in azo dye wastewater treatment. *J Clean Prod* 321:128971